Eur Biophys J (2002) 30: 571–587
DOI 10.1007/s00249-001-0186-y

ARTICLE

Nikolai I. Kiskin · David Ogden

Two-photon excitation and photolysis by pulsed laser illumination modelled by spatially non-uniform reactions with simultaneous diffusion

Received: 24 May 2001 / Revised version: 3 September 2001 / Accepted: 3 September 2001 / Published online: 19 October 2001

Abstract Two-photon absorption in the focus of a pulsed laser has the potential for localized photolysis of caged compounds, generating high concentrations of neurotransmitters, hormones and messengers. The concentrations of cage, intermediates and products in the femtolitre focal volume depend on reaction rates and diffusional exchange with the external volume. This problem of reaction with diffusion was analysed with analytical and numerical methods to determine simple relations between parameters useful in the design and interpretation of experiments. The diffraction-limited laser spot is approximated well by a sphere, radius A, in diffusional exchange with either an infinite uniform medium, representing extracellular photolysis, or within a non-permeable sphere, a ''cell'' of radius B, representing intracellular photolysis. Photolysis is modelled as sequential irreversible reactions, with either the excitation step alone, rate constant k_e, or with a subsequent ''dark'' reaction, rate constant k_p. For extracellular photolysis, steady-state depletion of a cage averaged in a spherical spot increases hyperbolically with k_e, with half-maximum depletion at $k_e = K_{0.5} = 2.5\ D/A^2$, where D is the diffusion coefficient. With measured parameters for spot size $A = 0.3$ μm and diffusion $D = 800$ μm^2/s, $K_{0.5} = 22{,}200$ s^{-1}. The optimal exposure for localized photolysis is the characteristic diffusion time $\tau = A^2/D$, 113 μs in this example, and is the time taken to reach 57% of steady state in the diffusion-limited case. In the two-step model, with excitation and ''dark'' reaction steps, rate constants both exceeding $K_{0.5}$ are necessary to generate 50% of maximal product concentration in the illuminated volume. High concentrations of photolysis products depend particularly on a high excitation rate constant ($k_e > K_{0.5}$), and localization of the products requires fast dark reactions ($k_p > K_{0.5}$). If products diffuse faster than the cage, their steady-state concentrations are decreased, and concentration transients may occur. For localized intracellular photolysis, the duration of exposure that generates product concentration at the cell boundary, B, less than 10% of the spot concentration should be shorter than $0.043(B/A)^3\tau$, and is determined by diffusion.

Keywords Multi-photon photolysis · Localized photolysis · Diffusion and reaction · Laplace transform

N.I. Kiskin[1] · D. Ogden (✉)
National Institute for Medical Research,
The Ridgeway, London, NW7 1AA, UK
E-mail: dogden@nimr.mrc.ac.uk
Tel.: +44-20-89593666 ext 2003
Fax: +44-20-89064477

Present address:
[1]Physiologisches Institut der Universität Freiburg,
79104 Freiburg, Germany

Introduction

Recent advances in instrumentation have led to the widespread use of laser light sources for high-resolution scanning imaging of biological tissues. By the use of pulsed near-infrared lasers, multi-photon excitation is restricted to femtolitre spot volumes around the laser focus and gives enhanced resolution and tissue penetration (Denk et al. 1990; Xu et al. 1996). It is anticipated that two-photon and multi-photon photolysis of ''caged'' biologically active compounds can improve the spatial resolution of ligand release to the level of single synapses or subcellular organelles (Denk 1994). Practical applications of two-photon methods show some successes, mostly in intracellular photolysis of caged Ca^{2+} (Lipp and Niggli 1998; Brown et al. 1999). At the same time, a number of studies have showed that the effective rates of product release for conventional ''caging'' groups are too low to be useful in two-photon applications (Brown et al. 1999; Furuta et al. 1999; Kiskin et al. 2001). Thus, to facilitate the development of new caged compounds and comparisons of photolysis reaction rates, an analysis of processes occurring during photolysis within the two-photon excitation spot is required. The volume of the two-photon spot is only a few

femtolitres, and is in diffusional exchange with the bulk solution on a sub-millisecond timescale comparable to or faster than reaction times for photolysis of many caged compounds (McCray and Trentham 1989; Corrie and Trentham 1993). The two-photon effect occurs only at very high light intensities, and to prevent damage to the biological sample and microscope optics, laser illumination is pulsed with femto- or picosecond pulses. With ~10 ns interval between the pulses, at a low efficiency of excitation, some time is required before the products of photolysis accumulate sufficient concentration within the spot and the spatial distribution is therefore influenced by diffusion. At the other extreme of very high efficiency of excitation, depletion of caged compound occurs within the spot and will slow down the photolysis, the process counteracted by diffusional influx of unphotolysed cage. As a result, the rate and localization of photolysis is strongly influenced by diffusion of reactants into and out of the reaction volume, and the relation between reaction rates and diffusion is analysed here.

Photolysis reactions are complex, beginning with light-dependent excitation of caged molecules followed by several "dark" steps before intermediates finally convert to photolysis products, each reagent subject to diffusion. The analysis presented here describes (1) the relation between light absorption and photolysis rate, (2) the role of diffusion of the cage and intermediates and (3) the optimum pulse duration which maximizes yield but minimizes the spatial spread of the products. Extracellular photolysis was modelled by diffusional exchange with an infinite bulk solution. By restricting boundary conditions to diffusion inside an impermeable sphere, models of intracellular photolysis are discussed in order to find additional constraints imposed by this experimental arrangement. Models were set up analytically where possible by solving the systems of diffusion equations in Laplace-transformed form (Carlslaw and Jaeger 1959; Crank 1975) with numerical inversion of the results. This has revealed some simple relations between diffusional and geometric parameters and reaction rates that can be applied more broadly than the results of numerical simulations. The kinetics of product concentration averaged in the two-photon spot can be measured and was analysed to give a theoretical background for practical two-photon and laser photolysis calibrations (see following paper, Kiskin et al. 2001). Part of the results has been presented earlier in abstract form (Kiskin and Ogden 1998).

Theory and models

Light absorption, quantum yield and rate constants in pulsed two-photon photolysis

The photolysis rate constants should first be linked to physical processes occurring when caged reagents are illuminated with pulsed laser light. The initial excitation is controlled by the light intensity and laser pulse parameters, and depends on the two-photon cross-section and quantum yield of the cage. Investigation of mechanisms in near-UV photolysis has shown that excitation is followed by one or more "dark" reactions that are often rate limiting (reviewed by McCray and Trentham 1989; Corrie and Trentham 1993). The photolysis reactions can be represented as sequential, irreversible reaction steps, with rates for each step independent of the product concentrations for that step, and conversion defined by rate constants and efficiency factors. The cage is illuminated by trains of sub-picosecond laser pulses arriving at regular intervals T. Two-photon photolysis proceeds during consecutive pulses as cage molecules absorb light and accumulate in intermediate states. The efficiency of light absorption, α, is the fraction of molecules in the illuminated volume (the laser "spot") which absorb two photons of incident light during a single laser pulse and is determined by the two-photon absorption cross-section of the cage, the light intensity and laser pulse parameters. The process of absorption is considered as an instantaneous event, and the quantum efficiency, $0 < \eta < 1$, is the probability of photolysis following absorption and accounts for the proportion of excited molecules, $1-\eta$, returning to the ground state before the next laser pulse arrives.

The rate constant for the excitation step, k_e, determines the rate of cage depletion and the rate at which intermediates that will finally decay to products are formed, and is given by the conversion per pulse times pulse frequency:

$$k_e = \alpha\eta/T \tag{1}$$

For photolysis of a caged compound with quantum efficiency $\eta = 1$ and infinitely fast "dark" reactions, the overall rate of photolysis is $k_e = \alpha/T$, determined only by excitation pulse parameters and the ability of the cage to absorb light with the two-photon effect. "Dark" reactions are generally not fast enough for this expression to give the rate of product formation, but it is valid for analysis of the rate of formation of the activated intermediate, E, and depletion of the cage, considered below.

Two-photon photolysis is usually produced by a focused laser beam, having a squared relation of the intensity with axial distance, z, and radius, r, in the focal volume. Two-photon excitation depends on the square of the intensity and has a fourth-power dependence on the geometric parameters r and z (Xu and Webb 1997; Kiskin et al. 2001). This produces a spatial gradient of α, and excitation proceeds with different rate constants, depending on the distance from the focus. A spatially non-uniform excitation rate constant k_e is designated as $k_e(r,z)$ in cylindrical coordinates, and the simplest model of photolysis can be written as:

$$C \xrightarrow{k_e(r,z)} E \tag{2}$$

In this formulation, E may represent either an excited intermediate, if only depletion of the cage C is considered, or the final product of photolysis if it is assumed that the "dark" conversion reaction is fast compared to the interpulse interval T.

In the second, more general formulation, "dark" reactions are included explicitly. Excited intermediate species E and product P are assumed, and the "dark" reactions are approximated by a single irreversible reaction with a rate constant k_p:

$$C \xrightarrow{k_e(r,z)} E \xrightarrow{k_p} P \tag{3}$$

Note that k_p is spatially uniform, as the second step proceeds wherever intermediate E diffuses. Furthermore, the reaction steps are assumed independent, and reactions of E are not influenced by light.

In this scheme the accumulation of product P in the spot during a train of laser pulses can be derived first without considering the effects of diffusion by taking a time interval sufficiently small for reactions not yet to be disturbed by diffusion (e.g. total time $t \approx 10$ μs), but long enough to contain a large number, N, of pulses, $N > 20$ ($t > 0.2$ μs). If β is the fraction of activated intermediate molecules E which converts to product P during the pulse period T, so $0 < \beta \leq 1$, the product concentration, P_N, found in the spot at the Nth pulse at time $t = (N-1)T$ (first pulse arrives at $t = 0$) is

determined by the fraction of molecules excited by previous pulses *and* converted to product by this time. The sum of P accumulated for all N pulses, normalized to initial cage concentration C_0, is given by:

$$P_N/C_0 = 1 - (1-\alpha\eta)^N - \alpha\eta(1-\beta)\left[(1-\alpha\eta)^N - (1-\beta)^N\right]/(\beta-\alpha\eta) \quad (4)$$

In the case of fast "dark" reactions where all of intermediate E converts to product during the pulse interval T (see above), so that $\beta = 1$, Eq. (4) reduces to $1-(1-\alpha\eta)^N$ which, for small $\alpha\eta$ and large N, and substituting for k_e from Eq. (1), gives the kinetics of product formation as $P(t) = C_0[1 - \exp(-k_e t)]$.

More usually, the timescale of the dark reactions is longer than the interpulse interval, $k_p \ll 1/T$, and β is small, so $\beta = 1 - \exp(-k_p t) \approx k_p t$. An expression in terms of the rate constants can be obtained by substituting in Eq. (4) the relation for k_e from Eq. (1) and the approximation for β. Further assuming small $\alpha\eta$ and $N \to \infty$, Eq. (4) becomes:

$$P(t)/C_0 = 1 - \left[k_p exp(-k_e t) - k_e exp(-k_p t)\right]/(k_p - k_e) \quad (5)$$

Thus, after a large number of pulses N the exact expression (Eq. 4) derived for pulsed illumination converges to that given by formal kinetics (Eq. 5) for the two-step scheme with continuous illumination, and is used in the analysis below of photolysis models containing both excitation and "dark" reactions. It should be noted, however, that for high values of k_p or $k_e \sim 1/T$ there could be small deviations in the initial kinetics at $N < 20$, where Eq. (5) gives an underestimate of results that are described adequately by Eq. (4). In the two-step scheme of Eq. (3) the overall rate of photolysis cannot be faster than the lower value of either k_p or k_e. Furthermore, it differs from the single-step reaction in showing a sigmoidal initial onset when the rate constants differ substantially and both are much less than $1/T$.

Localized photolysis with diffusion

Laser illumination in the focus of a microscope objective is spatially non-uniform and produces excitation rates that depend on position, creating concentration gradients, which in turn generate diffusional fluxes. These factors determine the kinetics at each point. An exact treatment for Gaussian-Lorentzian laser beam profiles requires the numerical solution of non-linear partial differential equations in cylindrical coordinates. However, simplified analytical approaches used here provide a better understanding of the factors affecting the efficiency of photolysis, they allow useful comparisons between models, and permit prediction of changes that will result from changes of photochemical or laser beam parameters.

Definition of models

Two diffusional models corresponding to different boundary conditions are considered: (1) extracellular photolysis – photolysis in a small spherical region, (radius $r = A$) with diffusion in an infinite volume of solution – or (2) intracellular photolysis – photolysis in a spherical region $r \le A$ inside a larger sphere of radius B. The formulations of the models are summarized in Table 1.

Differential equations

These can be written in spherical coordinates as:

$$\frac{D}{r^2}\frac{\partial}{\partial r}\left(r^2\frac{\partial C}{\partial r}\right) - k(r)C = \frac{\partial C}{\partial t} \quad (6)$$

for a single-step reaction (Eq. 2) with rate constant $k(r)$ (models PIM1, PIM1a, PSP1, RGS, RGC, RSP of Table 1), or for the two-step reaction based on Eq. (3) as a system of two equations:

$$\frac{D}{r^2}\frac{\partial}{\partial r}\left(r^2\frac{\partial C}{\partial r}\right) - k_e(r)C = \frac{\partial C}{\partial t} \quad (7)$$

$$\frac{D}{r^2}\frac{\partial}{\partial r}\left(r^2\frac{\partial E}{\partial r}\right) + k_e(r)C - k_p E = \frac{\partial E}{\partial t} \quad (8)$$

with the conversion E to P in the second step occurring in an infinite medium. The initial conditions are $C(r,0) = C_0$ for the cage, and reaction products are absent, so $P(r,0) = E(r,0) = 0$. For simplicity the same diffusion coefficient D is assigned to the cage, product and intermediate, and therefore the material balance condition can be used:

$$C(r,t) + E(r,t) + P(r,t) = C_0 \quad \text{for all } r \ge 0 \text{ and } t \ge 0 \quad (9)$$

In this case the distribution of C found from Eq. (6) defines the distribution of $E(r,t) = C_0 - C(r,t))$, and distributions of C and E

Table 1 Models describing photolysis (first-order reactions) or zero-order release with diffusion

Model	Description	Reaction(s)	Rate constant(s)	Diffusion of reagents
PIM1	Photolysis reaction in the spot with diffusion in infinite medium	$C \to E$ inside the sphere $r \le A$	k	In an infinite medium
PIM1a	Photolysis reaction on the surface of well-mixed sphere with diffusion in infinite medium	Surface condition $4\pi A^2 D\frac{\partial C}{\partial r} = \frac{4\pi}{3}A^3 kC$	k	"Instant" diffusion inside the sphere $r \le A$; at $r > A$, diffusion in an infinite medium
PSP1	Photolysis reaction in the spot, diffusion inside impermeable sphere, radius B	$C \to E$ inside the sphere $r \le A$	k	Inside the sphere $r \le B$
PIM2	Photolysis reaction in the spot with finite speed of product formation	$C \to E$ inside the sphere $r \le A$; $E \to P$ in an infinite medium	k_e k_p	In an infinite medium
RSP	Constant speed release inside the sphere	$\partial E/\partial t = \begin{cases} K & \text{at } r \le A \\ 0 & \text{at } r > A \end{cases}$	$K = kC_0$	In an infinite medium
RGS	Constant speed release with geometry of a "Gaussian sphere"	$\partial E/\partial t = K\exp\left(-r^2/w_R^2\right)$	$K = kC_0$	In an infinite medium
RGC	Constant speed release with geometry of a "Gaussian cylinder"	$\partial E/\partial t = K\exp\left(-r^2/w_R^2\right)\exp\left(-z^2/w_Z^2\right)$	$K = kC_0$	In an infinite medium

found from Eqs. (7) and (8) uniquely define the distribution of product P.

Excitation profiles

Three spatial profiles of excitation were used to approximate the profile of two-photon excitation in the laser spot. In the first, the geometry of the laser spot was simplified to a small sphere of radius $r = A$ illuminated with uniform light intensity and situated in an infinite medium. The photolysis reaction has a first-order rate constant k everywhere inside the sphere but does not occur outside it. Since the sphere differs only in that it is illuminated, reagents can diffuse freely without restrictions at the border of the sphere, and concentration functions and their first derivatives on the radius inside and outside the sphere are set equal on the boundary $r = A$. Additional boundary conditions state that the concentrations of cage and products are finite at $r = 0$ and $r \to \infty$.

Two spatial profiles were used to approximate better the distribution of squared light intensity in the laser focus but are considered only with zero-order kinetics, i.e. constant rate of release of E as a function of position. One is continuous release in a "Gaussian sphere" (RGS model, Table 1), approximating the diffraction-limited laser spot obtained when a high numerical aperture microscope objective is strongly overfilled by the incident laser beam, with spatial distribution described by:

$$\partial E/\partial t = K \exp\left(-r^2/w_R^2\right) \quad K = C_0 k(0) \tag{10}$$

The other approximates the case of an underfilled objective, where the geometry of the intensity-squared illumination in the focus is a Gaussian-Lorentzian function, which in cylindrical coordinates can be approximated by a "Gaussian cylinder" function:

$$\partial E/\partial t = K \exp\left(-r^2/w_R^2\right) \exp\left(-z^2/w_Z^2\right) \tag{11}$$

with $w_Z > w_R$ so that the profile is extended on the z-axis (RGC model, Table 1).

All three profiles were evaluated with superposition of continuous sources (Carslaw and Jaeger 1959; Crank 1975), which permits solution of the diffusion equation for any release geometry by integrating diffusion from point or surface sources. In these models the changes in reaction rate due to depletion of the cage C at high excitation rates were neglected, and the concentration of product E at any point is proportional to the rate constant K. Although analytical evaluation taking account of depletion and diffusional changes is possible (see Brünger et al. 1985), the results are complicated and less easily applied.

Methods of solution and definition of parameters

The Laplace transform is a standard method for the solution of equations arising from problems of reaction constrained within a sphere, as discussed in Carslaw and Jaeger (1959) for heat transfer in spherically symmetric composite media. Making the substitution $V(r,t) = rC(r,t)$ in Eqs. (7) and (8) and applying the Laplace transform with parameter p gives:

$$v1(r,p) = r\int_0^\infty C1(r,t)e^{-pt}dt \quad v2(r,p) = r\int_0^\infty C2(r,t)e^{-pt}dt \tag{12}$$

for cage concentration inside ($v1$, $C1$) and outside the sphere of radius A ($v2$, $C2$). Since different processes occur in these regions, substitution of the transforms in Eq. (6) with the initial conditions gives a system of two second-order differential equations in r:

$$\frac{d^2v1}{dr^2} - v1\frac{k+p}{D} = -\frac{C_0 r}{D} \quad (r < A) \tag{13}$$

$$\frac{d^2v2}{dr^2} - v2\frac{p}{D} = -\frac{C_0 r}{D} \quad (r > A) \tag{14}$$

The boundary conditions imposed on $v1$, $v2$ at $r = 0$, $r = A$, $r \to \infty$ or $r = B$ (intracellular photolysis) follow from those for $C(r,t)$ given above. These equations and, where appropriate, additional equations for intermediate E, were solved, the results converted back to Laplace transforms of concentration, analysed, and timecourses found by numerical inversion.

Concentrations averaged over the two-photon volume

The two-photon volume approaches the dimensions of synapses and intracellular organelles that might be investigated experimentally with local concentration changes, so it is appropriate to consider concentrations averaged over this volume. For example, the averaged concentration of the product of photolysis E in a single step reaction $C \to E$ (model PIM1 Table 1) is defined by:

$$E_{av}(t) = 3/A^3 \int_0^A E(r,t)r^2 dr \tag{15}$$

and the total amount of E generated in time t:

$$M(t) = 4\pi \int_0^\infty E(r,t)r^2 dr \tag{16}$$

If the diffusion coefficients are equal, these quantities are equal to the cage concentration depleted from the spot and the total cage consumed in time t in an infinite medium, respectively. Thus, the concentration of the cage averaged over the two-photon volume can be found as $C_{av}(t) = C_0 - E_{av}(t)$. Evaluation of the timecourses requires inversion of the Laplace transforms for solutions of Eqs. (13) and (14).

In the steady state, the averaged concentration in the spot, $E_{sp} = \lim_{t\to\infty} E_{av}(t)$, and the radial distribution, $E_{ss}(r) = \lim_{t\to\infty} E(r,t)$, can be found analytically, either by using the property of the Laplace transform $F(p)$ of function $f(t)$:

$$\lim_{t\to\infty} f(t) = \lim_{p\to 0}[pF(p)] \tag{17}$$

(McCollum and Brown 1965), or by solving Eqs. (7) and (8) with partial derivatives on time equal to zero.

For the constant release models with the rate defined by Gaussian sphere or cylinder functions, the average concentrations of E, or by substitution C, were found from the concentration distributions by integration in an infinite medium and normalization to the spot volume:

$$E_{av}(t) = \frac{4\pi}{V_s}\int_0^\infty E(r,t)r^2 dr \tag{18}$$

where V_s is the spot volume, for the geometries considered here equal to $4\pi A^3/3$ for uniform intensity in a sphere, $\pi^{1.5} w_R{}^3$ in a Gaussian sphere profile (model RGS of Table 1) and $\pi^{1.5} w_R{}^2 w_Z$ in a Gaussian cylinder profile (model RGC).

The results for intracellular photolysis (model PSP1), with spot photolysis and diffusion inside the larger sphere $r \le B$, are more complicated mathematically, and solutions were analysed numerically.

All calculations were performed in MathCad 6.0e Plus for Windows (MathSoft, USA) with Origin 5.0 (Microcal, USA) for graphical output. The numerical algorithm for MathCad implementing the Laplace transform inversion using the Padé approximation (a rational approximation with polynomials of 8–10 degree) was presented by Faouzi Amar at http://www.mathsoft.com/mathcad/library/education/ilaplace.mcd. The algorithm produced less than 1% error in numerical tests using examples from the table of Laplace transforms for diffusional problems, superior to direct calculations in the numerical evaluation of large exponents.

Results

Extracellular photolysis

Single-step photolysis in a well-mixed spherical volume and diffusional exchange with an infinite external medium (model PIM1a of Table 1)

If the cage is photolysed in a single-step irreversible reaction with an excitation rate constant k, the depletion of the cage can be analysed as a function of k by the methods of Carslaw and Jaeger (1959). Additionally assuming that the reagents are always well mixed inside the photolysis sphere $r \le A$, the concentrations on the surface of the sphere of the cage $C(A,t)$ or the first product $E(A,t)$ are equal to uniform concentrations inside the spot, and the photolysis reaction is regarded as occurring only on the surface at $r = A$. Diffusion in an infinite medium as a result of photolysis in this case is essentially the model of radiation from a spherical surface into an infinite medium (Carslaw and Jaeger 1959; eq. 9.10.3). The boundary condition for $C(r,t)$ at $r = A$ equates fluxes due to diffusion through the surface to the reaction inside the sphere and can be written in the form of Fick's diffusion law:

$$4\pi A^2 D\frac{\partial C}{\partial r} = \frac{4\pi}{3}A^3 kC\,, \text{ or } \frac{\partial C}{\partial r} = hC \tag{19}$$

where $h = kA/(3D)$. The analytical solution (Carslaw and Jaeger 1959; modified eq. 9.10.3) is:

$$C(r,t) = C_0 - \frac{C_0 kA^2}{3DrH}\left\{\operatorname{erfc}\frac{r-A}{2\sqrt{Dt}} - \exp\left[H(r-A)+H^2Dt\right]\operatorname{erfc}\left(\frac{r-A}{2\sqrt{Dt}}+H\sqrt{Dt}\right)\right\} \tag{20}$$

Making the substitution $)E(r,t) = C_0 - C(r,t))$ for the product of the reaction gives:

$$E(r,t) = \frac{C_0 kA^2}{3DrH}\left\{\operatorname{erfc}\frac{r-A}{2\sqrt{Dt}} - \exp\left[H(r-A)+H^2Dt\right]\operatorname{erfc}\left(\frac{r-A}{2\sqrt{Dt}}+H\sqrt{Dt}\right)\right\} \tag{21}$$

where $H = 1/A + kA/(3D)$ and $\operatorname{erfc}(x) = 1 - \operatorname{erf}(x)$. An asymptotic approximation for the function $e^x\operatorname{erfc}(x^{0.5})$ at large x (Carslaw and Jaeger 1959; appendix II) allows solutions at large values of time:

$$C(A,t\to\infty) = \frac{3C_0}{3+k\tau} \times \left[1 + \frac{k\tau}{\pi^{0.5}(3+k\tau)}\left(\frac{\tau}{t}\right)^{0.5} - \frac{9k\tau}{2\pi^{0.5}(3+k\tau)^3}\left(\frac{\tau}{t}\right)^{1.5} + O\left(t^{-2.5}\right)\right]$$
$$E(A,t\to\infty) = \frac{C_0 k\tau}{3+k\tau} \times \left[1 - \frac{3}{\pi^{0.5}(3+k\tau)}\left(\frac{\tau}{t}\right)^{0.5} + \frac{27}{2\pi^{0.5}(3+k\tau)^3}\left(\frac{\tau}{t}\right)^{1.5} + O\left(t^{-2.5}\right)\right] \tag{22}$$

where $O(t^{-2.5})$ is a remainder term that decreases with time as $t^{-2.5}$ and can be neglected at large t. The characteristic time $\tau = A^2/D$ defines a time constant that measures how quickly the concentration changes on a spatial scale of radius A as a result of diffusion (the "relaxation time"; Cussler 1997). Values of D and A can be assigned as follows. For amino acids at 20 °C, aqueous diffusion coefficients are 1064 $\mu m^2/s$ for glycine, 910 $\mu m^2/s$ for α-alanine (Weast 1989), 760 $\mu m^2/s$ for glutamine (Longsworth 1953) and for proteins in the range of 7–130 $\mu m^2/s$ (Altman and Dittmer 1972). A diffusion coefficient in a free medium of $D = 800$ $\mu m^2/s$ has been used for neurotransmitters when modelling synaptic processes (Clements 1996) and will be used here. Measurements of the focused laser beam in our experiments (see Kiskin et al. 2001) showed that a radius $A = 0.3$ μm for a sphere would include the half-maximum of squared light intensity distribution in the focus in the specimen plane orthogonal to the optical axis. With these values of $D = 800$ $\mu m^2/s$ and $A = 0.3$ μm, the value of τ is 113 μs.

Equation (22) gives the main conclusion of this model: in the steady state the normalized concentration of the cage in the sphere follows a hyperbolic dependence on reaction rate constant k, $C(A,\infty) = 3C_0/(3+k\tau)$. Half-maximal depletion of the cage in the steady state on the surface and inside the sphere will be achieved at a reaction (excitation) rate of $k = 26{,}700$ s^{-1}.

Photolysis and diffusion within the two-photon sphere in an infinite medium (model PIM1 of Table 1)

The assumption of uniform concentration within the spherical volume of photolysis gives good results at times approaching the steady state, but is less accurate at distances $r \sim A$ and in the initial stages of reaction. If the assumption of well-mixed spot concentrations is abandoned, the model yields more precise results at early times. The rate constant for photolysis excitation is assumed constant in the spherical region $r \le A$. However, diffusional fluxes occur within the spot and between the region of photolysis and the external medium, and the resulting concentration gradients of the cage give rise to different reaction rates inside the spot. The solution of ordinary differential equations (Eqs. 13 and 14) in the Laplace transform may be averaged over the two-photon volume to give the transform of the average concentration of the cage for a reaction with rate constant k and $\tau = A^2/D$:

$$C_{av}(p,k) = \frac{3C_0 k\left(1+\sqrt{p\tau}\right)}{p[(k+p)\tau]^{1.5}\left[\sqrt{p}\tanh\sqrt{(k+p)\tau}+\sqrt{k+p}\right]} \times \left[\sqrt{\tau} - \frac{\tanh\sqrt{(k+p)\tau}}{\sqrt{k+p}}\right] + \frac{C_0}{k+p} \tag{23}$$

The last term of this equation is the Laplace transform of the solution for cage depletion without diffusion, $C_0\exp(-kt)$. Inversion of Eq. (23) gives the kinetics of

the average cage concentration in the two-photon volume, $C_{av}(t)$. Figure 1A shows the results of calculations with k equal to 0.1, 1 or 10 times $K_{0.5}$, where $K_{0.5}$ is the rate constant of the reaction which in the steady state depletes the cage to 50% of C_0, and is equal to $2.5/\tau$ as described below. With $\tau = 113$ μs the timecourse of $C_{av}(t)$ (solid lines) initially follows the kinetics of the reaction without diffusion (dotted lines) and reaches a non-zero steady state (horizontal arrows). In the steady state, the cage is continuously consumed inside the spot, with diffusional influx of unphotolysed cage maintaining a steady concentration. Figure 1A shows that for slow photolysis reactions the steady-state depletion is small, and at high photolysis rates the cage concentration is not depleted to zero. Furthermore, with the representative values of A and D used for the calculation, the timecourse of cage depletion and product generation approaches a steady state on a millisecond timescale.

Solution in the steady state

From Eq. (23), the averaged concentration of cage in the spot in the steady state, C_{sp}, equals:

$$C_{sp}(k) = 3C_0(k\tau)^{-1.5}\left(\sqrt{k\tau} - \tanh\sqrt{k\tau}\right) \quad (24)$$

Figure 1B presents the values of C_{sp} calculated from Eq. (24) for reactions with different rate constants k (points). Use of the Padé approximation for the function $\tanh(x)/x$ (see Smith 1985 for methods) shows that $3[x - \tanh(x)]/x^3 = 5/(5 + 2x^2) + O(x^6)$, where $O(x^6)$ can be neglected. Thus, from Eq. (24) the normalized depletion of the cage inside the spot in the steady state has a hyperbolic dependence on the rate constant of the reaction, k:

$$C_{sp}(k)/C_0 \approx \frac{2.5}{2.5 + k\tau} = \frac{1}{1 + k/K_{0.5}} \quad (25)$$

Here, $K_{0.5} = 2.5/\tau = 2.5D/A^2$ is the rate constant that generates 50% cage depletion in the steady state. Figure 1B shows that the approximation given by Eq. (25) (solid line) is very close to the exact result given by Eq. (24) (points). With the values of A and D of 0.3 μm and 800 μm^2/s used here, $K_{0.5}$ has a large value, 22,200 s^{-1}; it varies in proportion to the diffusion coefficient and spot sizes in proportion to $1/A^2$. Note that Eqs. (23)–(25) depend explicitly on neither A nor D; the scaling of the results is determined by k and $\tau = A^2/D$. The kinetics and steady-state values of the average concentrations, $E_{av}(t)$ or $E_{sp}(k)$, can be obtained by subtracting the values of $C_{av}(t)$ or $C_{sp}(k)$, respectively, from the total cage concentration C_0, making the assumption that the reagents have the same diffusion coefficient.

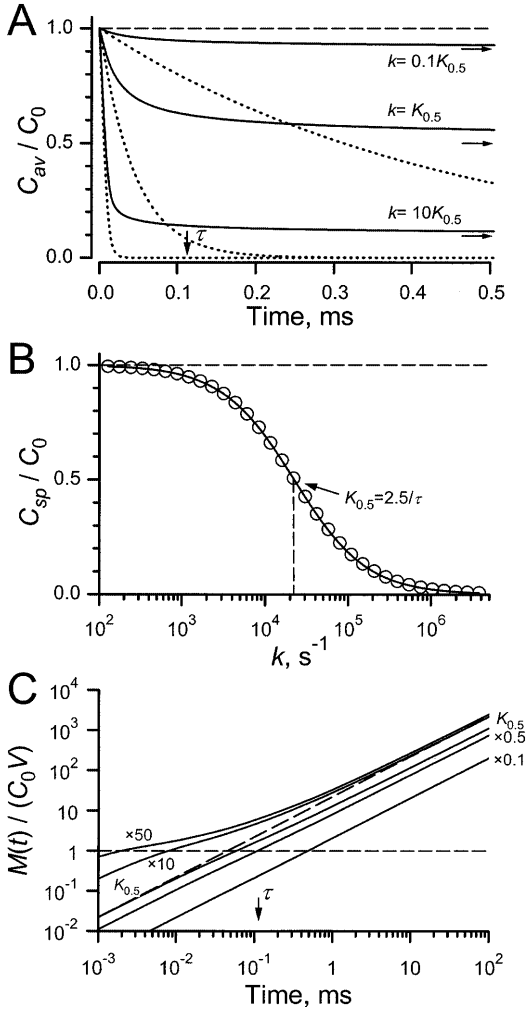

◄

Fig. 1A–C Timecourse and steady-state levels of cage depletion by photolysis. Single irreversible reaction in the two-photon volume (sphere, radius $A = 0.3$ μm) with diffusion in an infinite medium (Table 1, model PIM1). Data normalized to initial cage concentration C_0 (**A**, **B**) or amount of cage in the spot volume C_0V (**C**). Diffusion parameters $D = 800$ μm^2/s and $A = 0.3$ μm, yielding characteristic diffusional time $\tau = A^2/D = 113$ μs (indicated by *vertical arrows* in **A** and **C**). **A** Kinetics of average cage concentration in the two-photon spot (*solid lines*) for a first-order irreversible reaction with rate constants $k = K_{0.5}$, $0.1K_{0.5}$ or $10K_{0.5}$. Data derived by numerical inversion of the Laplace transform in Eq. (23); steady-state values C_{sp}/C_0 defined by Eq. (24) are indicated by *horizontal arrows*: 0.503, 0.909 and 0.0960, respectively. For comparison, exponential timecourses calculated for spatially uniform reactions with the same rate constants shown by *dotted lines*. **B** Steady-state average concentration of cage remaining in the two-photon volume at rate constant k (abscissa, logarithmic scale). *Points* represent exact analytical solution (Eq. 24), the *solid line* shows its simplified form $1/(1 + k/K_{0.5})$ (Eq. 25). Rate constant $K_{0.5} = 2.5/\tau = 22{,}200$ s^{-1} corresponds to the reaction which in the steady state depletes 50% of cage in the spot (*vertical dashed line*). **C** Total amount of cage photolysed up to time t, $M(t)$, in an infinite medium at different reaction rate constants k (indicated in multiples of $K_{0.5}$ near corresponding curves). $M(t)$ found by integration of Eq. (23) with Laplace transform inversion and normalized to the initial amount of cage, C_0V, in the two-photon volume V (*horizontal dashed line*). Double-logarithmic plot. Limiting steady-state cage consumption is shown by *dashed line*, slope $k_{ef} = K_{0.5}$. Reactions with $k > K_{0.5}$ show an initial high rate of consumption and approach the limiting steady-state rate asymptotically as the cage is depleted from the spot. At $k \le K_{0.5}$, the consumption rate shows little change

The physical significance of the rate constant $K_{0.5}$ is illustrated by considering the kinetics of *total* cage conversion integrated over an infinite medium. The total amount of cage $M(t)$ converted to E over time t, normalized by the initial amount of cage in the reaction sphere C_0V, was calculated by numerical inversion and plotted in Fig. 1C for reactions with different rate constants k in units of $K_{0.5}$ and spot volume $V = 4\pi A^3/3 =$ 0.113 fL for $A = 0.3$ μm. In these calculations, $K_{0.5} = 22{,}200$ s^{-1} as above. With $k > K_{0.5}$ the rate of conversion initially decreases substantially with time; in contrast, for $k \ll K_{0.5}$ the rate decreases insignificantly. Linear slopes at early times $t \ll \tau$ ($\tau = 113$ μs) represent initial rates of reaction not affected by diffusion, when $M(t) \approx C_0Vkt$. At late times, $t > \tau$, the slopes decrease because the cage in the spot becomes depleted by photolysis and thus the rate of reaction becomes limited by diffusional replacement of the cage. At a high rate constant, $k \gg K_{0.5}$, the slowing of the reaction rate due to cage depletion is pronounced; in the extreme case $k = 50K_{0.5}$ there is initially complete depletion of the cage in the spot (in Fig. 1C, crossing the horizontal dashed line, which represents the spot content C_0V) followed by reaction at a rate limited by the rate of diffusional cage influx. This time to deplete the spot represents for fast reactions ($k > 10^5$ s^{-1}) the most favourable duration of the photolysing laser pulse train, $NT \leq \tau$, the time when photolysis is almost complete within the spot, but the products remain localized.

The constant rate of cage depletion in the steady state (data at $t > \tau$ in Fig. 1C) is seen by integrating Eq. (23) and using the properties of the Laplace transform. The constant steady-state rate defines an effective rate constant, k_{ef}, in the relation $M(t \rightarrow \infty) = k_{ef}C_0Vt$. The same rate of cage consumption can be expressed from Eq. (25) in terms of the microscopic reaction rate constant k as $kC_{sp}Vt$ from the expression for the steady-state average concentration C_{sp}. Equating these definitions, the effective steady-state rate constant k_{ef} and microscopic reaction rate constant k have the relation:

$$\frac{1}{k_{ef}} = \frac{1}{k} + \frac{1}{K_{0.5}} \tag{26}$$

For slow reactions with $k \ll K_{0.5}$, the value of k_{ef} is close to k because there is little cage depletion (lower curves, Fig. 1C), and at $k \gg K_{0.5}$ the effective steady-state rate constant k_{ef} has a maximum equal to $K_{0.5}$ (dashed line and top curves, Fig. 1C). For fast reactions (as $k \rightarrow \infty$), $K_{0.5} = 2.5D/A^2$ is the limiting rate of photolysis in the steady state, determined by the rate with which cage molecules diffuse into the spot to replace those photolysed.

As the value of $K_{0.5}$ limits the steady-state photolysis rate by fast reactions, the maximum rate of cage consumption by steady-state photolysis in an infinite medium amounts to $C_0VK_{0.5} = 2.51C_0$ pmol/s (with units of C_0 in mol/L and $V = 0.113$ fL as above). This quantity is dependent only on diffusion and, for a spherical spot, will vary in proportion to AD. This small rate of steady-state cage consumption and product generation at maximal photolysis rate illustrates that two-photon laser microphotolysis cannot produce large quantities of photolysis products, and that direct calibration by chemical measurements is difficult because too little cage consumption or product formation occurs for analysis. Furthermore, the results show that prolonging the time of laser illumination beyond approximately $NT = \tau$ does not change the reactant concentrations in the spot, and increasing the photolysis rate constant k_e at high laser power is progressively less effective in changing the reactant concentrations in the spot at times approaching the steady state. These factors must be considered in designing and interpreting experiments.

Summary of results for single-step excitation

The results for cage depletion in a single excitation step show the dominant role of diffusional exchange on the reaction rates in regions with sub-micron dimensions. For realistic diffusion coefficients, 100–800 μm^2/s, the characteristic time constant of exchange for a 0.6 μm diameter spot is $\tau = A^2/D = 900$ μs to 113 μs, respectively. The excitation rate constant for 50% cage depletion in the steady state is estimated as $K_{0.5} = 2.5/\tau = 22{,}200$ s^{-1} with a 0.6 μm diameter spot and $D = 800$ μm^2/s. The rate of photolysis in the steady state is limited to a maximum of $K_{0.5}$ by diffusional replacement of the cage even at high excitation rate constants, and the optimum laser exposure at high excitation rates is $t \approx \tau$, to achieve near steady-state concentration with minimal spread of products away from the spot. The diffusional loss of intermediates from the spot also requires, by the same considerations of diffusion, that rates of conversion in the "dark" reactions have $k_p > K_{0.5}$ for localization of products in the vicinity of the laser spot.

Kinetics of concentration changes in the two-photon spot

The kinetics of the photolysis reaction is determined by the reaction rate constants, diffusional replacement of the cage and diffusional loss of the intermediates and products from the spot. Simple analytical solutions cannot be found for the kinetics of reaction with diffusion in terms of the reaction rate constant and diffusional time constant. However, numerical analysis of the models with spherical geometry for the two-photon spot leads to some useful empirical relations given here.

The analytical solution for reaction on the surface of a sphere immersed in an infinite medium (model PIM1a of Table 1) can be used to interpret the diffusional τ in relation to the timecourse of the concentration change in the spot. According to Eq. (21), at time $t = \tau$, slow reactions ($k \rightarrow 0$) will produce an average concentration of product in the spot E_{sp} equal to 1–e × erfc(1) = 0.572 of

that in the steady state. A similar result arises when considering zero-order release in a sphere (model RSP of Table 1; see Eq. 35 below): the reaction at time $t = \tau$ gives $1 - 3\pi^{-0.5} + 1.5\mathrm{erf}(1) = 0.571$ of the steady-state concentration. Thus, the time, $t_{0.57}$, when 57% of the steady-state concentration is achieved can be used to evaluate the effects of the excitation rate constant and diffusional parameters on the kinetics of the averaged spot concentrations. This was applied to the model analysed above, with first-order reactions resulting from uniform illumination of the spherical spot and diffusional gradients of concentration within the spot and bulk solution (model PIM1 of Table 1). $t_{0.57}$ was calculated for reaction rate constants, k, and diffusion conditions, $\tau = A^2/D$, by numerical inversion of the Laplace transform (Eq. 23). The results are plotted in Fig. 2 (closed circles) as the dependence of $t_{0.57}$ on reaction rate constant k for a 100-fold range of τ from 11.3 μs to 1.13 ms, corresponding to $K_{0.5}$ values of 2220 to 222,000 s^{-1}.

At slow reaction rates ($k \ll K_{0.5}$), $t_{0.57}$ is determined by diffusion and is equal to τ. With reaction rate constants $k \geq K_{0.5}$, the $t_{0.57}$ time decreases, and at $k \gg K_{0.5}$ becomes inversely proportional to k, following conventional diffusion-independent kinetics. The simplest empirical description of the numerical results presented in Fig. 2 is the relation:

$$\frac{1}{t_{0.57}} = k + \frac{1}{\tau}, \quad \text{or} \quad t_{0.57} = \tau/(1 + k\tau) \tag{27}$$

showing that diffusion and reaction influence the kinetics in parallel. Figure 2 (solid line) shows that this approximation is close to the calculated times (points) except for small deviations at the highest values of k, where $1/t_{0.57}$ equals $1.1k$ to $1.14k$. Thus, if at different k the timecourse and steady-state concentrations are known, Eq. (27) allows the estimation of diffusion and reaction parameters from $t_{0.57}$. In this context, $t_{0.57}$ can serve as a characteristic time constant describing the kinetics of the reaction with diffusion localized to a sphere.

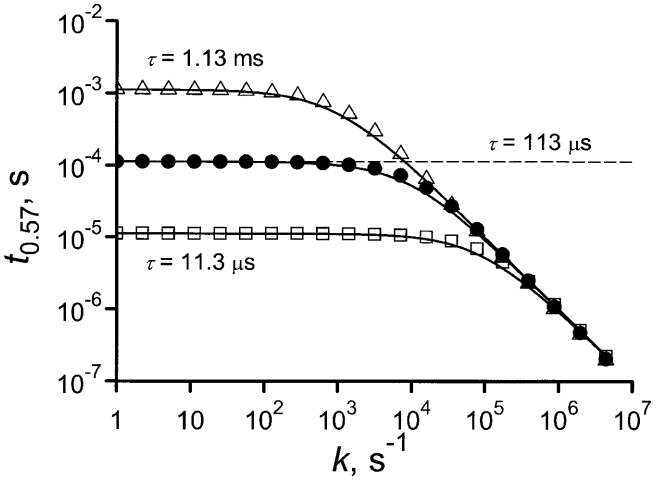

Fig. 2 The time, $t_{0.57}$, when the concentration of product of a single reaction averaged over the spot (Eq. 2; PIM1 model of Table 1) reaches 57% of the steady-state value. $t_{0.57}$ values were calculated numerically from Eqs. (23) and (24) and plotted against the reaction rate constant k. Points are calculated for different diffusion time constants $\tau = A^2/D$. *Filled circles*: $\tau = 113$ μs; *triangles*: $\tau = 1.13$ ms, corresponding to slow diffusion and/or large spot radius; *squares*: time constant $\tau = 11.3$ μs, fast diffusion and/or small spot radius. *Solid lines* show empirical approximations calculated with Eq. (27), $t_{0.57} = \tau/(1 + k\tau)$. *Horizontal dashed line* shows $\tau = 113$ μs ($A = 0.3$ μm, $D = 800$ $\mu m^2/s$)

Sequential excitation and release reactions with diffusion (model PIM2 of Table 1)

The contributions of the excitation and "dark" reaction rate constants to the overall rate of photolysis and distribution of products was investigated by considering two sequential irreversible reactions described earlier (Eq. 3):

$$C \xrightarrow{k_e(r)} E \xrightarrow{k_p} P \tag{28}$$

The return of a proportion of intermediate E to the ground state rather than decaying to product P is assumed to be faster than the interpulse interval T, and is thus accounted for as a quantum yield factor in the excitation rate constant k_e (see Eq. 1). The cage, intermediates and products are freely diffusing, the excitation (k_e) is confined to the laser spot, a sphere of radius A, and the "dark" reactions of product release (k_p) can occur in the whole medium from excited state intermediates E. This model was solved with the approximation of spherical geometry and equal diffusion coefficients for all reagents. The average steady-state concentration, P_{sp}, of final product in the spot is:

$$P_{sp}/C_0 = 1 + \frac{1}{k_e - k_p} \times \left\{ \frac{k_p}{1 + k_e/K_{0.5}} - \frac{k_e}{1 + k_p/K_{0.5}} 0.5\left[1 + \exp\left(-2\sqrt{k_p\tau}\right)\right] \times \left[1 + \sqrt{k_p/k_e}\tanh\left(\sqrt{k_e\tau}\right)\right] \right\} \tag{29}$$

As in Eqs. (24) and (25), the Padé approximation was used, and $\tau = A^2/D$ and $K_{0.5} = 2.5/\tau$ have the same values as before. Numerical calculations (not shown) confirmed that the results obtained using Eq. (29) were close to those obtained without use of the approximation from the complete expression for the two-step reaction (model PIM2 of Table 1). Figure 3 shows steady-state concentrations of the product P calculated in four limiting cases, ascribing fixed "fast" ($10K_{0.5}$) or "slow" ($0.1K_{0.5}$) values to either rate constant k_e or k_p and plotting the average concentration in the spot as a function of the other variable rate constant. With a fast rate of product formation, $k_p = 10K_{0.5}$, the steady-state concentration of product depends hyperbolically on the excitation rate constant k_e (Fig. 3, solid line) as described by Eq. (25)

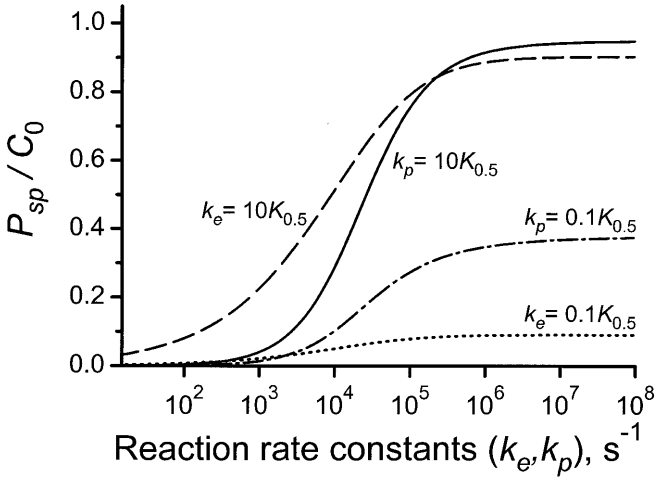

Fig. 3 Photolysis by two sequential irreversible reactions: excitation with the rate constant k_e inside the spot and product formation in an infinite medium with "dark" reaction rate constant k_p. Reaction scheme Eq. (3), PIM2 model of Table 1. Normalized steady-state product concentrations averaged in the spot, P_{sp}/C_0, calculated from complete expression in model PIM2 (Eq. 29 gives its simplified form). Spot radius $A = 0.3$ μm, diffusion coefficient $D = 800$ μm^2/s. Limiting cases of fixed rate constants: *solid line*: fast "dark" conversion, $k_p = 10K_{0.5}$; *dashed line*: fast excitation, $k_e = 10K_{0.5}$; *dash-dot line*: slow "dark" conversion, $k_p = 0.1K_{0.5}$; *dotted line*: slow excitation, $k_e = 0.1K_{0.5}$ are shown plotted against the variable rate constant, k_e or k_p

for a single-step reaction. With $k_e = 10K_{0.5}$, i.e. at fast excitation, the steady-state concentration of product P in the spot depends on k_p as a quasi-hyperbolic function (Fig. 3, dashed line), and 50% of the initial cage concentration is photolysed at lower rates of k_p than found for k_e in the reverse situation (Fig. 3, solid line). In the case of low excitation rates, low concentrations of intermediate will be found in the two-photon volume because of losses by diffusion, and therefore little product is formed at any value of k_p (Fig. 3, dotted line). Data show that even with a slow "dark" reaction (Fig. 3, dash-dot line) it is possible to obtain significantly more product by increasing the excitation rate than in the reverse situation of slow excitation and increasing k_p (Fig. 3, dotted line). Thus, fast k_e produced by efficient excitation in each laser pulse increases the overall product concentration by producing large concentrations of intermediate E in the excitation volume. More generally, the dependence of steady-state concentration on both reaction rates (Eq. 29) demonstrates that high rate constants of *both* reactions $\geq K_{0.5}$ are required in order to generate high concentrations of photolysis product P inside the spot. In practice, k_e is determined by the two-photon photolysis cross-section and the intensity of the pulsed illumination, and is to that extent an experimental variable, although at present two-photon cross-sections are generally too low to be useful at non-toxic laser intensities. The rate constant k_p is determined by the photochemical properties of the cage and is an equally important parameter that cannot be varied in an experiment.

Spatial distribution of intermediates and products

Single reaction step

The distribution of photolysis products will be determined by the rate of breakdown of the intermediates produced by excitation in the laser spot in relation to their diffusion into the bulk solution. In the limiting case when the intermediates are short lived, represented by a fast "dark" reaction rate constant $k_p \gg 1/T$, the distribution of product E complements cage depletion and follows the $1/r$ rule of steady-state distribution with distance in the bulk solution (Carslaw and Jaeger 1959; Crank 1975). For the model of a well-mixed reaction in the sphere (Eqs. 21 and 22), the steady-state ratio of concentration at radius r to the concentration on the surface of the sphere equals A/r. Analytical solution for the model with diffusional gradients within the sphere shows that the steady-state concentration at $r > A$ changes with radius also in proportion to A/r, multiplied by a dimensionless function of the reaction rate constant $[x^3 - x^2\tanh(x)]/\{x^3 - 3[x - \tanh(x)]\}$, where $x = (k\tau)^{0.5}$. This function depends slightly on reaction rate constant, increasing from 0.83 at $k \leq K_{0.5}$ to 0.95 at $k = 100K_{0.5}$, up to the limit of 1 at infinite k. Thus, for the single-step models, the steady-state distribution of concentrations outside the spot is determined by diffusion and decays with increase in radius as A/r, with little dependence on the rate of reaction.

Two sequential reactions

The spatial distributions of product $P(r)$ and intermediate $E(r)$ that result from different rates of either excitation or photolytic conversion were calculated and plotted as the radial concentration distributions, shown in Fig. 4. These were calculated for $A = 0.3$ μm and $\tau = A^2/D = 113$ μs at times equal to 0.1τ, τ, 10τ and in the steady state, and rate constants k_e and k_p were set as fast, $10K_{0.5}$, or slow, $0.1K_{0.5}$. Two cases are considered: slow excitation and fast photolysis (Fig. 4A) and the reverse situation of fast excitation and slow photolysis (Fig. 4B). Note the different concentration ranges (ordinate scales) required to compare the spatial spread. The distributions of $E(r)$ (Fig. 4A, B, left panels) show that setting k_e high or low has little effect: the distribution of E remains confined to the two-photon volume, though with much smaller amplitude at low excitation rates and slightly wider profile at slow photolysis. The concentration of E increases in proportion to the rate k_e and reaches a steady state slowly after an initial overshoot at $t > \tau$ (seen particularly in Fig. 4B). Additionally, it was noted that large differences of excitation and photolysis rates can produce transient depletion of E in the centre with local maxima on the periphery of the two-photon volume (not shown). These effects are analogous to depletion in the centre of the spot,

predicted for two-photon excitation of fluorescence analysed in the presence of bleaching or dye saturation (Xu and Webb 1997).

The spatial distribution of product $P(r)$ does not display transient behaviour and differs markedly in the two limiting cases shown in Fig. 4A, B (right panels). Figure 4A confirms that the case of very fast "dark" reactions is similar to a single reaction with the overall rate defined by excitation k_e. However, the same is not true for the opposite case of a slow "dark" reaction rate constant. The steady-state amplitude is greater at fast k_e and slow k_p (Fig. 4B), but the distribution is broader than in the reverse case. This larger steady-state concentration is achieved slower than at other rate settings (indicated by the larger displacement between curves for 10τ and steady state in Fig. 4B). Despite fast excitation and a higher final concentration of product than in Fig. 4A, the diffusional spread of excited intermediate E, resulting from low k_p, generates a spatial product distribution considerably wider than for a single-step reaction or reactions with slow excitation and fast photolysis (Fig. 4A). The differences are more pronounced at times $t > \tau$ and in the steady state. This effect can be verified with the analytical expression for the steady-state dependence of product concentration on radius for $r > A$, which, on letting $k_e \to \infty$, at $k_p << K_{0.5}$ simplifies to:

$$P_{ss}(r) = C_0 A/r\left[1 - \exp\left(-r\sqrt{k_p/D}\right)\sinh\left(\sqrt{k_p\tau}\right)/\sqrt{k_p\tau}\right] \quad (30)$$

The exponential dependence on radius in this expression decays with spatial constant $(D/k_p)^{0.5}$, which decreases the concentration in the vicinity of the spot and increases the distal concentration relative to the A/r decay for the single reaction step.

The spatial distribution of the product can be characterized by the half-maximal radius at which the product concentration equals 50% of that in the centre of the spot. Figure 5A shows the timecourse of the change of this measure during photolysis by two sequential reactions (model PIM2 of Table 1). For fast excitation and a slow "dark" reaction ($k_e = 10K_{0.5}$, $k_p = 0.1K_{0.5}$, solid line), there is a considerably greater

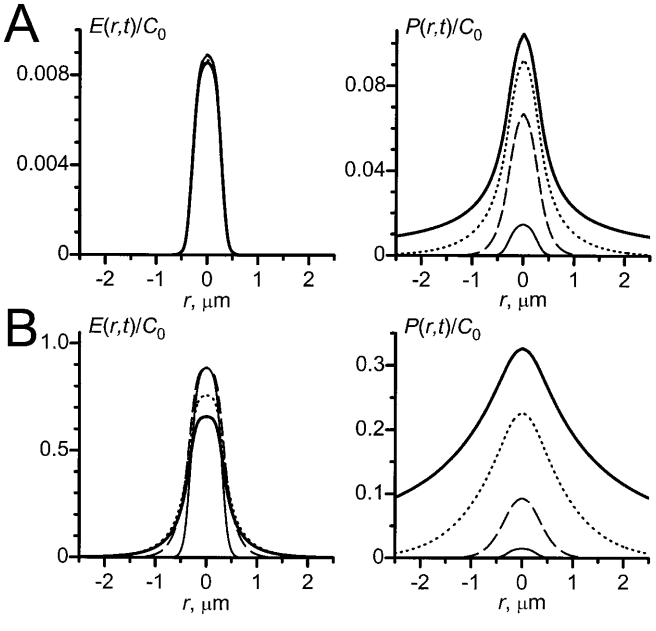

Fig. 4A, B Spatial concentration profiles of intermediate E (*left panels*) and final product P (*right panels*) for two sequential irreversible reactions (model PIM2 of Table 1). Concentrations normalized to initial cage concentration C_0 and plotted against radius r for different times of reaction equal to 0.1τ (*thin solid lines*), τ (*dashed lines*), 10τ (*dotted lines*) and in the steady state (*thick lines*). Different ordinate scales chosen to facilitate comparison. **A** Slow excitation ($k_e = 0.1K_{0.5}$) and fast "dark" conversion ($k_p = 10K_{0.5}$). **B** Fast excitation ($k_e = 10K_{0.5}$) and slow "dark" conversion ($k_p = 0.1K_{0.5}$)

Fig. 5 Spatial distribution of product concentration characterized by radius at half-maximum, at different reaction times (**A**, **C** and **D**) and in the steady state for different reaction rate constants (**B**). **A** Radii at half-maximal product concentration for two sequential reactions (model PIM2 of Table 1) are plotted against reaction time for fast excitation and slow "dark" reaction ($k_e = 10K_{0.5}$, $k_p = 0.1K_{0.5}$) (*solid line*) and in the reverse situation ($k_e = 0.1K_{0.5}$, $k_p = 10K_{0.5}$) (*dashed line*). **B** Steady-state radii of half-maximal product P concentration in this model plotted against the rate constants of "dark" reaction k_p, data for two fixed rate constants of excitation: fast $k_e = 10K_{0.5}$ (*solid line*) and slow $k_e = 0.1K_{0.5}$ (*dashed line*); double-logarithmic plots. The value of $K_{0.5} = 22{,}200\ s^{-1}$ is shown on the abscissa scale by an *arrow*. **C** Timecourse of radius of half-maximal product concentration calculated for the zero-order release models with geometries of a Gaussian cylinder (RGC model, cylinder dimensions $w_R = 0.35$ μm, $w_Z = 2.47$ μm, *solid line*) or a Gaussian sphere (RGS, $w_R = 0.35$ μm, *dashed line*). For the cylindrical model the radius of the spot in the focal plane (surface $z = 0$) is analysed. **D** For the RGC model the same analysis as in **C** is performed for the half-maximal spread of the product distribution along the optical axis (line $r = 0$). The half-width of the axial distribution is plotted on the same ordinate scale as in **C** with 1.7 μm offset to facilitate comparison

spatial spread of the distribution with time when compared to the reverse situation of slow excitation and fast "dark" conversion ($k_e = 0.1K_{0.5}$, $k_p = 10K_{0.5}$, dashed line). Figure 5B shows the dependence of the half-maximal radii in the steady state (asymptotic values of curves in Fig. 5A) on the rate constant k_p, presented for two fixed values of k_e, fast ($10K_{0.5}$, solid line) and slow ($0.1K_{0.5}$, dashed line). The graphs show that when the "dark" reaction is slow, $k_p < K_{0.5}$, the half-width is exclusively determined by k_p independently of k_e, and the limiting slope as $k_p \to 0$ is proportional to $(k_p)^{-0.5}$, as implied in the expression given above. At large $k_p > K_{0.5}$, the spatial distribution is narrow, though slightly wider at high excitation rate k_e (Fig. 5B, solid line) than at slow k_e (dashed line), comparable to the single-step reaction. Figure 5B also shows that rate constants of "dark" reactions of 100–500 s^{-1} typical for nitrophenylethyl cages (McCray and Trentham 1989; Corrie and Trentham 1993) would result at any excitation rate in half-maximal radii of product distribution in the range 2.4–4.8 μm in the steady state, extending the radial dimensions of release 8 to 16 times those of the two-photon spot.

Gaussian excitation profiles

The spatial distribution of the product E of a single-step reaction was also studied for excitation with Gaussian spot geometry, either spherically symmetrical (RGS), expected for an overfilled objective, or cylindrical (RGC), corresponding to an underfilled objective, with a constant photolysis rate proportional to the intensity squared. The values of $w_R = 0.35$ μm for both and $w_Z = 2.47$ μm for the cylinder (see Table 1) were chosen so that the half-maximal radius in the focal plane equals $A = 0.3$ μm and the half-maximal width of the spot on the z axis for RGC model is 4.11 μm, values that match those of a squared Gaussian-Lorentzian distribution for a focused laser beam with waist 0.7 μm. Figure 5C shows that in the focal plane the Gaussian sphere profile (dashed line) produces a product distribution comparable to the reaction in the uniformly illuminated sphere (Fig. 5A, dashed line). However, the radial broadening of the Gaussian cylinder distribution with time (Fig. 5C, solid line) is much greater and may be due to the larger reaction volume in the Gaussian cylinder. In the axial direction, the Gaussian cylinder distribution undergoes broadening with a similar timecourse, reaching larger dimensions than that seen in the focal plane (Fig. 5D). The results in Fig. 5C, D were calculated for single-step zero-order release reactions, and it is likely that with two sequential first-order reactions with a Gaussian cylinder excitation profile the effect of a slow "dark" reaction in spreading the released product outside the ellipsoidal illuminated spot would be even more pronounced.

Single-step reaction with different diffusion properties of the cage C and product E

When the diffusion coefficients of the cage and the other reagents generated are different, the condition of material balance at each point is no longer valid, and the concentrations need not be complementary to C_0. Considering a single reaction step, the system of equations for C and the first intermediate E (Eqs. 7 and 8) can be solved with diffusion coefficients different for each, D_C and D_E. This may occur, for instance, if E is a smaller molecule than C, and consequently $D_C < D_E$. With this modification, the steady-state depletion of the cage occurs as described above (Eqs. 24 and 25 with $D = D_C$), but the average concentration of the product E differs and is described using same approximations as in Eqs. (24) and (25) by:

$$E_{sp}(k)/C_0 = \frac{D_C}{D_E}\frac{1}{1 + K_{0.5}/k} \tag{31}$$

with $K_{0.5}$ equal to $2.5D_C/A^2$. The steady-state concentration of E in the spot thus follows the steady-state depletion of cage C multiplied by the factor D_C/D_E. For illustration, Fig. 6A shows the steady-state average concentration of product in the spot $r \le A$ ($A = 0.3$ μm) as a function of the reaction rate constant k, when E diffuses with 4 times greater D than the cage, with $D_E = 4D_C = 800$ $\mu m^2/s$ (solid line), and, for comparison, curves calculated with both species diffusing either like the cage with $D = D_C = 200$ $\mu m^2/s$ (dotted line) or like the product, $D = D_E = 800$ $\mu m^2/s$ (dashed line). At small values of k the product concentration follows the curve with the diffusion coefficient for the product, D_E, but at higher reaction rates ($k > K_{0.5}$) has the average steady-state level decreased by the ratio D_C/D_E (0.25 in this example).

The kinetics of the average product concentration in the spot, $E_{av}(t)$, can be evaluated for unequal diffusion coefficients using the Laplace transform. These were calculated and plotted for different reaction rate constants (in multiples of $K_{0.5} = 2.5D_C/A^2 = 5560$ s^{-1}) in Fig. 6B. Also plotted for comparison are curves at reaction rate constants $k = 2.5D/A^2$ with both diffusion coefficients set to either D_C (200 $\mu m^2/s$, dotted line) or to D_E (800 $\mu m^2/s$, dashed line). Initially, $t < A^2/D_E$, the timecourse at $D_E = 4D_C$ is as if both diffusion coefficients were set to D_E; later a smaller steady-state level (E_{sp}) is achieved when the diffusion coefficients are different. At high reaction rates, $k > K_{0.5}$, the initial rise is faster and the kinetics show clear transient peaks greater than the steady state, occurring in less than 100 μs, followed by a slow decline to the steady-state level, due to faster diffusion of E from the spot. The amplitude of the transient is larger and the peak occurs earlier at high k. The timecourse with equal diffusion coefficients always showed monotonic increases of product in the spot which followed the cage depletion, as in Fig. 1A. Thus, as a result of differences in diffusion coefficient, continuous laser photolysis can produce submillisecond

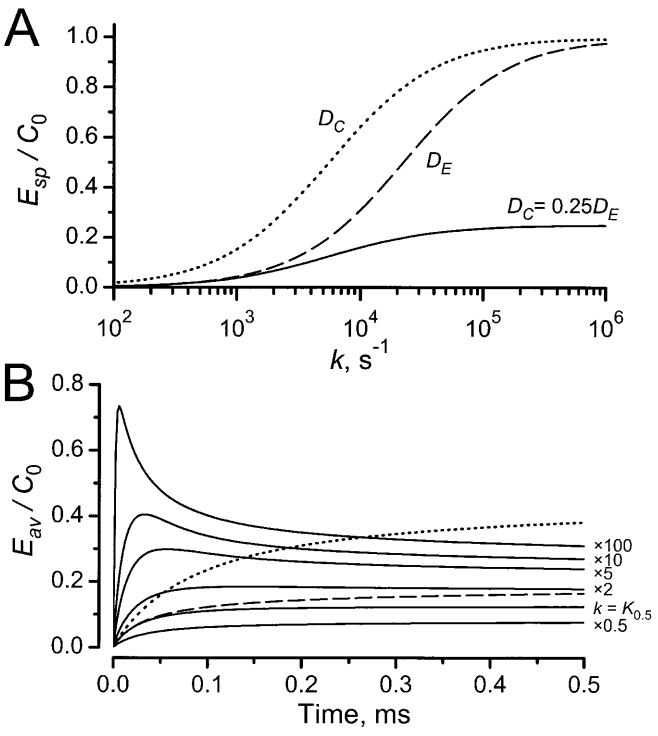

Fig. 6 Different diffusion coefficients for cage and product E in single-step photolysis (PIM1 model of Table 1); effects of different reaction rates k on average product concentration in the spot in the steady state (**A**) and its transient kinetics (**B**). Results calculated for spot radius $A = 0.3$ μm with four-fold difference in diffusion coefficients for cage ($D_C = 200$ μm^2/s; $K_{0.5} = 2.5D_C/A^2 = 5560$ s^{-1}) and product ($D_E = 800$ μm^2/s). **A** Steady state, normalized concentrations of product averaged over the spot, E_{sp}/C_0, plotted against rate constant k for chosen different diffusion coefficients (*solid line*) and for identical diffusion coefficients for cage and product equal to D_E (*dashed line*) or D_C (*dotted line*). Semi-logarithmic coordinates. **B** Kinetics of average concentration of product E in the spot (normalized to C_0) for four times different diffusion coefficients of cage and product. *Continuous lines*: timecourses calculated with rate constants indicated on the curves in multiples of $K_{0.5} = 5560$ s^{-1}. Note that the traces for $k > K_{0.5}$ display transiently high concentrations of E with decay to the steady state. For comparison, the kinetics calculated for equal diffusion coefficients are shown for $D = D_E = 800$ μm^2/s (*dashed line*) and $D = D_C = 200$ μm^2/s (*dotted line*); reaction rates are set to $2.5D/A^2$

initial "spikes" of high product concentration, and the amplitude of these spikes can transiently reach C_0 (i.e. complete photolysis).

Determination of k and τ from asymptotic approach to the steady state

It has been noted that solutions for various diffusion problems in an infinite medium approach the steady state with an asymptotic increase or decrease of concentration proportional to $t^{-0.5}$ (Crank 1975). The possibility that this property exists for the averaged concentrations and might be useful in evaluating k and τ by extrapolation, thereby avoiding long laser exposures, was tested with analytical solutions for the models listed in Table 1. It was found that extrapolation of data with short laser exposures plotted in $1/\sqrt{t}$ coordinates can be used to estimate the steady-state level if exposures are longer than $\tau = A^2/D$.

The procedure can be described for a single-step reaction in an infinite medium (PIM1 model of Table 1) and equal diffusion coefficients for C and E. By analogy with Eq. (22) the asymptotic approximation of $E_{av}(t)$ for large $t \to \infty$ will have the form:

$$E_{av}(t) = E_{sp} + Sl(k,\tau)t^{-0.5} + O(t^{-1.5}) \tag{32}$$

where the asymptotic slope Sl is a function of k and τ, but not t. Sl is identified by applying the Laplace transform to the right side of this expression, multiplying by p (the transform parameter) and comparing the result with the solution for the model in the Laplace transformed form $E_{av}(p,k,\tau)$, also multiplied by p and expanded in a series in p at $p \to 0$. From the properties of Laplace transforms (see Theory and models), terms independent of p form the steady-state concentration E_{sp}, while equating the terms of the order $\sim\sqrt{p}$ we can find the slope Sl. This procedure applied to the single-step reaction, with the use of Eq. (25), gives:

$$\begin{aligned} E_{av}(t \to \infty) &= E_{sp} + \frac{k\tau(C_0 - E_{sp})^2}{3C_0}\left(\frac{\tau}{\pi t}\right)^{0.5} + O(t^{-1.5}) \\ &\approx E_{sp}\left[1 - \frac{5}{6(1 + k/K_{0.5})}\left(\frac{\tau}{\pi t}\right)^{0.5} + O(t^{-1.5})\right] \end{aligned} \tag{33}$$

Numerical calculations of the kinetics with a reversed transform in Eq. (23) confirm that the approximation is valid for large values of $t \gg \tau$. Thus, plotting the timecourse of average concentration in $t^{-0.5}$ coordinates yields an asymptotic line intercepting the ordinate at the steady-state value E_{sp} as $t \to \infty$. This intercept allows the steady-state concentration and asymptotic slope to be found graphically. After this, theoretical expressions for the asymptotic slope defined by Eq. (33) and for the steady-state concentration (Eq. 25) can be used to estimate the unknowns, k and τ.

For two sequential reactions (PIM2 model of Table 1), this method gave an approximation relating the slope, Sl ($Sl < 0$), and the steady-state average concentration of final product, P_{sp}, by the equation:

$$Sl/(P_{sp} - C_0) \approx \frac{5}{6}\left(\frac{\tau}{\pi}\right)^{0.5} \frac{1}{1 + K_{0.5}/k_e} \tag{34}$$

Although both Sl and P_{sp} are complicated functions of both rate constants k_e and k_p, this relation does not explicitly depend on the rate constant k_p and together with Eq. (29) allows the determination of two parameters from the set of k_e, k_p and τ from the steady-state results, provided the remaining parameter is determined independently.

Finally, for the constant-release rate models, the steady-state and asymptotic values at $t \to \infty$ can be found directly from the model solutions. A constant rate

of release in the sphere radius A (model RSP of Table 1) gives average concentrations of product E in the sphere and the asymptotic approach to the steady state as:

$$\begin{aligned} E_{\mathrm{RSP}}(t) &= Kt - 0.4K\frac{t^{0.5}}{\pi^{0.5}\tau^{1.5}}\left(\tau^2 - 3t\tau + 2t^2\right)\exp(-\tau/t) \\ &\quad +0.8K\frac{t^{2.5}}{\pi^{0.5}\tau^{1.5}} - 2K\frac{t^{1.5}}{\pi^{0.5}\tau^{0.5}} \\ &\quad -0.2K(5t-2\tau)erfc\left[(\tau/t)^{0.5}\right] \\ &= \frac{K\tau}{2.5}\left(1 - \frac{5\tau^{0.5}}{6\pi^{0.5}t^{0.5}} + \frac{5\tau^{1.5}}{60\pi^{0.5}t^{1.5}}\right) + O\left(t^{-2.5}\right) \end{aligned} \quad (35)$$

The result is consistent with the single-step reaction given above when $k \ll K_{0.5}$ and no cage depletion occurs in the spot, in which case Eq. (25) also gives the steady-state value $kC_0/K_{0.5} = K\tau/2.5$, and the same $t^{-0.5}$ slope as that given by Eq. (33).

For the Gaussian sphere with the product release rate defined as $K\exp(-r^2/w_{\mathrm{R}}^2)$ and diffusional time constant $\tau = w_{\mathrm{R}}^2/D$ (model RGS in Table 1), the average concentration has the timecourse:

$$\begin{aligned} E_{\mathrm{RGS}}(t) &= 2^{-1.5}K\tau\left(1 - 1/\sqrt{1+2t/\tau}\right) \\ &= 2^{-1.5}K\tau\left[1 - (\tau/2t)^{0.5} + 0.5(\tau/2t)^{1.5}\right] + O\left(t^{-2.5}\right) \end{aligned} \quad (36)$$

The slope of the initial increase of the product concentration averaged over the spot is $K/2^{1.5}$, ~2.8 times slower than the reaction rate $K(r=0)$ in the focal centre. At large times, asymptotic behaviour when plotted in $t^{-0.5}$ coordinates holds, as for the other models.

For product release within a Gaussian cylinder (RGC model of Table 1), the derivation, results and asymptotic behaviour are given in the following paper (Kiskin et al. 2001; see Appendix). Briefly, the expression for average product concentration in the spot with characteristic radial and axial diffusion time constants $\tau_{\mathrm{R}} = w_{\mathrm{R}}^2/D$ and $\tau_{\mathrm{Z}} = {w_{\mathrm{Z}}}^2/D$ is given by:

$$\begin{aligned} E_{\mathrm{RGC}}(t) &= 2^{-1.5}K\tau_{\mathrm{R}}\sqrt{\frac{\tau_{\mathrm{Z}}}{\tau_{\mathrm{Z}} - \tau_{\mathrm{R}}}} \\ &\quad \times \ln\left[\frac{\left(\sqrt{\tau_{\mathrm{Z}}} + \sqrt{\tau_{\mathrm{Z}} - \tau_{\mathrm{R}}}\right)\left(\sqrt{\tau_{\mathrm{Z}} + 2t} - \sqrt{\tau_{\mathrm{Z}} - \tau_{\mathrm{R}}}\right)}{\sqrt{\tau_{\mathrm{R}}(\tau_{\mathrm{R}} + 2t)}}\right] \end{aligned} \quad (37)$$

The derivative of E_{RGC} on time at $t \to 0$ is $K/2^{1.5}$, as for the Gaussian sphere model. An asymptotic expansion for large times is:

$$\begin{aligned} E_{\mathrm{RGC}}(t \to \infty) &= \frac{2^{-1.5}K\tau_{\mathrm{R}}}{\sqrt{1 - \tau_{\mathrm{R}}/\tau_{\mathrm{Z}}}}\ln\left(\frac{1 + \sqrt{1 - \tau_{\mathrm{R}}/\tau_{\mathrm{Z}}}}{\sqrt{\tau_{\mathrm{R}}/\tau_{\mathrm{Z}}}}\right) \\ &\quad - 0.25K\tau_{\mathrm{R}}\sqrt{\frac{\tau_{\mathrm{Z}}}{t}} + \frac{K\tau_{\mathrm{R}}}{48}\left(1 + 2\frac{\tau_{\mathrm{R}}}{\tau_{\mathrm{Z}}}\right)\left(\frac{\tau_{\mathrm{Z}}}{t}\right)^{1.5} + O\left(t^{-2.5}\right) \end{aligned} \quad (38)$$

The first term of the expansion represents the steady-state value, depending on the shape of the spot, and the result displays $t^{-0.5}$ kinetics as equilibrium is approached.

Intracellular photolysis: two-photon spot inside an impermeable sphere of radius B (model RSP1 of Table 1)

For intracellular microphotolysis, the volume where the product accumulates is determined by the size of the cell (or other physiological compartment) and, although generally larger, may be comparable with the dimensions of the laser spot. As a result, the diffusional redistribution of the reagents inside this closed volume has an influence on the timecourse of the reaction. The analysis considers a single, irreversible first-order reaction with rate constant k inside the sphere $r \le A$ with diffusional exchange limited to a larger concentric volume, $r \le B$, impermeable to both cage C and product E. From considerations discussed above, this approximation describes photolysis in the case of very fast "dark" reactions when the rate k of photolysis is equal to the excitation rate constant k_{e}.

At early times, $t \le \tau$, the presence of the outer shell at $r = B$ does not influence the course of the reaction, which initially behaves as if in an infinite medium. At the other extreme, in the steady state, all the cage inside the larger volume $r \le B$ ("the cell") will be photolysed by the irreversible reaction. Thus photolysis will be localized near the laser focus only for a limited time after the beginning of exposure. Considering these processes, the optimal duration of photolysis, when the reaction can still be practically regarded as localized to the spot, can be estimated.

Figure 7A shows for the single-step reaction the timecourses of the average spot concentration of the product E, released in $r \le A$ with rate constant $k = K_{0.5} = 22{,}200\ \mathrm{s}^{-1}$ and diffusing in an infinite medium (solid line) or inside impermeable spheres ("cells") of radius $B = 3$ μm and 6 μm (dashed lines). As expected, initially the average concentration of E in the two-photon spot follows the same curve as in the infinite medium. However, in the restricted volumes with long exposures $t > \tau$, the concentration inside the spot continues to rise even after the steady state is reached in the infinite medium. This rise is slower, and E_{av} finally approaches C_0, complete photolysis. In the limit of a very slow reaction compared to diffusion, the kinetics will be $E(r,t) = E_{\mathrm{av}}(t) = C_0[1 - \exp(-kA^3/B^3t)]$, i.e. the reaction is a uniform cage depletion over the whole cell slowed down by the factor $(A/B)^3$, the ratio of the two-photon volume to the impermeable volume. Also of interest are the concentrations on the boundary of the cell, at $r = B$ (Fig. 7A, dotted lines). These gradually increase with time after a delay which is longer for the larger of the two spheres, $B = 6$ μm. Note that the slow increase of concentration on the cell periphery (dotted lines) is seen

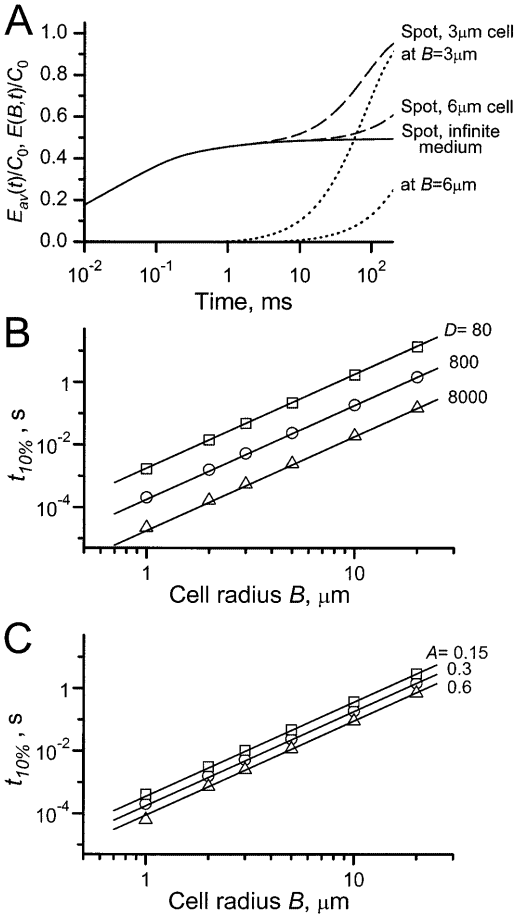

Fig. 7A–C Kinetics of product E distribution for a single-step reaction proceeding in the spot radius A concentric within impermeable spheres ("cells") of radius B (PSP1 model of Table 1). **A** Comparison of the timecourse of average concentration of product E in the spot for reaction in an infinite medium (PSP1 model of Table 1, *solid line*) with corresponding kinetics for reactions inside 3 and 6 μm radius cells (*dashed lines*); semi-logarithmic plot. For the PSP1 model, product concentrations on the boundary $r = B$ are shown by *dotted lines*. Radius of spot $A = 0.3$ μm, diffusion coefficient $D = 800$ μm^2/s, rate constant $k = K_{0.5} = 22{,}200$ s^{-1}. **B** The times $t_{10\%}$ when product concentration on the boundary of the cell reaches 10% of average product concentration in the spot are plotted against cell radius B for diffusion coefficients D of 80 μm^2/s (*squares*), 800 μm^2/s (*circles*) and 8000 μm^2/s (*triangles*). D (in μm^2/s) is indicated near the corresponding curves; spot radius $A = 0.3$ μm. **C** The dependence on cell radius B of $t_{10\%}$ values for $D = 800$ μm^2/s and reactions proceeding in spots of different radii A equal to 0.15 μm (*squares*), 0.3 μm (*circles*) and 0.6 μm (*triangles*). In **B** and **C** the rate constants of the reactions are set to corresponding values of $K_{0.5} = 2.5D/A^2$, and all *solid lines* are drawn in double logarithmic coordinates according to the approximating equation $t_{10\%} = mB^3/(AD)$. The estimate of m determined by regression on B for all data points is 0.0430 ± 0.0003

when the concentration inside the release spot $r \leq A$ (dashed lines) significantly deviates from the curve for an infinite medium (solid line). At later times, both curves approach each other and ultimately C_0 as the cage inside the cell is photolysed completely.

The times when photolysis is still considered localized can be defined by the time, $t_{10\%}$, when the concentration of product on the boundary reaches 10% of its average concentration in the spot, $E(B, t_{10\%}) = 0.1E_{av}(t_{10\%})$. At $t < t_{10\%}$, the concentration of product on the boundary will not exceed 10% of that in the spot, while at $t > t_{10\%}$ the product on the boundary will increase with a rate comparable to that inside the spot. $t_{10\%}$ times are plotted in Fig. 7B and C against the cell radius B for reaction with rate constant $k = K_{0.5}$ and for different diffusion conditions. The $t_{10\%}$ values displayed very weak dependence on the rate constant of the reaction, k: in the range of k from $0.1K_{0.5}$ to $10K_{0.5}$, $t_{10\%}$ values varied at $B > 1$ μm by less than 11%. An analytical expression for $t_{10\%}$ was not derived; however, all the numerical results obtained on changing the diffusion coefficient D by a factor of 10 (Fig. 7B) or radius of the spot A by two-fold (Fig. 7C) displayed slopes close to 3 when plotted against the cell radius, B, in double logarithmic coordinates. Analysis of the dependence on A and D suggested that $t_{10\%}$ times are proportional to the quantity $B^3/(AD) = (B/A)^3\tau$, which has the dimensions of time. The dependence on B^3 was confirmed when these data were scaled by the factor AD, pooled, and all-point regression on radius B in logarithmic coordinates gave a slope equal to 2.98 ± 0.08. From this fit, the optimal exposure times can be determined by the approximate empirical formula $t_{10\%} \approx 0.0430(B/A)^3\tau$ (Fig. 7B and C, all solid lines), valid over the range $A = 0.15$–0.6 μm and $D = 80$–8000 μm^2/s and for reaction rate constants $k = (0.25\text{–}25)D/A^2$. There were small deviations from this relation towards shorter times for $B \approx A$ at high reaction rates. The results can be extended for cells of any shape, provided the radius B represents the smallest distance between the spot and the cell boundary. Furthermore, the analysis shows that $t_{10\%}$ times are mainly determined by diffusion. Calculation with $A = 0.3$ μm and $D = 800$ μm^2/s, for a representative cell radius $B = 10$ μm, gives a value of $t_{10\%} = 179$ ms, a much longer exposure than the diffusional $\tau = 113$ μs characterizing exchange of the spot with an infinite medium. At the other extreme for $B = 3$ μm, $t_{10\%} = 4.84$ ms, closer to the diffusional τ. Thus, the results obtained in small cells with intracellular two-photon photolysis using pulses of 10–100 ms duration (e.g. Lipp and Niggli 1998) should be considered with caution, since considerable filling of the cell with products may occur by diffusion in this time, and effects seen cannot be ascribed to local actions on the basis of the two-photon effect.

Discussion

In experiments with laser microphotolysis it is important to know the factors affecting the concentration and timecourse of the photolysis products in the laser spot and the surrounding solution. Instrumental parameters such as laser intensity, spot size and pulse width and frequency can be controlled, but the efficiency and rates of photolysis are affected by intrinsic photochemical parameters. These are shown to be important in relation

to diffusional exchange of reactants in determining the extent and spatial distribution of product generation. The models presented here were formulated to discuss (1) the role of photochemical properties of the cage, the two-photon cross-section, quantum yields and "dark" reaction rate constants in reactions triggered by excitation with a pulsed, rather than continuous, laser source; (2) the influence of diffusion coefficients and spot geometry on the concentration and kinetics of the cage, intermediates and products, soon after the start of photolysis and in the steady state; and (3) the effect of limiting the volume of diffusion to a small region outside the spot, to simulate photolysis in a small cell or other restricted space. The levels of pulsed irradiation that can be applied in a physiological context and the resulting photolysis are assessed in the following paper (Kiskin et al. 2001).

Evidence from near-UV flash photolysis indicates that photolysis reactions can be generalized as two sequential, irreversible steps, the first requiring absorption of light to generate excited intermediates, a proportion of which proceed to decay in "dark" reactions to products independent of illumination. At a particular level of pulsed irradiation the proportion, α, of molecules excited by two-photon absorption during each laser pulse and the quantum efficiency η of the first step are properties of the cage which when averaged for laser pulses with frequency $1/T$ determine the rate constant of excitation, $k_e = \alpha\eta/T$. The influence of pulsed rather than continuous illumination on the kinetics of photolysis shows a difference only when a substantial proportion of the cage is excited by a single laser pulse and the exposure $t = NT$ has $N < 20$. The analysis of diffusional exchange between the two-photon spot and the external medium gives the optimal exposure approximately equal to the characteristic time $\tau = A^2/D \approx$ 100–200 μs, corresponding to $N > 10{,}000$.

In the laser spot, α is proportional to the two-photon cross-section of absorption, σ, and squared photon flux. The relation between the excitation rate constant, the cross-section of the two-photon photolysis $\delta = \sigma\eta$ and the instrumental parameters is derived in the following paper (Kiskin et al. 2001). Experimental assessment of the dependence of k_e on laser average power has permitted calculation of δ for conventional cages to be less than 0.1 GM (1 GM = 10^{-50} cm^4 × s/photon), a low value compared to, for example, fluorophores, resulting in very low rates of excitation at non-phototoxic light intensities, and in agreement with other published estimates. Thus, for photolysis calibration, values of k_e at different laser powers can be estimated either by measuring the accumulation of products with repetitive laser exposures short enough to avoid diffusional complications, or from the kinetics of reaction with diffusion by using the models and approaches described here. Because of the small amounts of product accumulated in the repetitive exposure measurements (the calculated rate of cage depletion is limited to $2.51C_0$ pmol/s in the steady state), the kinetic methods utilizing fluorescence detection can provide useful information. The results of two-photon photolysis calibrations with a caged fluorophore, in relation to phototoxicity in a synaptic preparation, are discussed in the following paper (Kiskin et al. 2001).

The influence on localized photolysis of diffusional exchange with a large volume was investigated by analytical and numerical solution of problems simplified to uniform photolysis excitation in a sphere, radius A. The average depletion of the cage by the photolysis reaction in the steady state was shown to have a hyperbolic dependence on the excitation rate with 50% depletion at $k_e = K_{0.5} = 2.5D/A^2$, where D is the diffusion coefficient for the cage. At low excitation rates the reaction proceeds with little cage depletion, whereas at high rates, steady-state photolysis cannot proceed faster than the cage is replaced in the spot by diffusion. The maximum effective rate constant, in the steady state, is limited by cage influx to be equal to $K_{0.5}$. This rate depends only on geometry and diffusion, and may be used to classify photolysis reactions as "slow" or "fast", depending on the concentration differences they can maintain in the spot. Furthermore, the kinetics of the initial depletion of the cage at low reaction rates ($k_e \ll K_{0.5}$) are determined by diffusional exchange with a characteristic time constant $\tau = A^2/D$. Numerical simulations showed that this is the time taken for the reaction to proceed to 57% of the steady-state level. This time also determines the optimal duration of photolysis, at which most of the photolysis product is still at the release site (Fig. 5). For small molecules diffusing freely in aqueous solution, τ is in the range of approximately 100–900 μs, and prolongation of the photolysis beyond τ does not substantially increase the local concentration, but spreads the reactants produced, both intermediates and products, by diffusion into the adjacent solution. The localization of photolysis products P depends on the extent of diffusion of intermediates E before the final reaction is complete, and therefore depends on the rate of "dark" reactions relative to diffusion. The parameter $K_{0.5}$, calculated for the diffusion of intermediates rather than the cage, determines the rates required. When "dark" reaction rates k_p are small relative to this quantity, calculations show that substantial broadening of the spatial distribution of product occurs, up to 8–16 times the spot radius, uninfluenced by the rate of the first excitation step k_e.

The difference of the results obtained between a uniformly illuminated sphere and a spherical Gaussian photolysis profile was not large: constant rate release models, RSP and RGS respectively, showed similar average concentrations in the spot. However, the simulations with the Gaussian cylinder profile, extended in the z-axis (RGC), showed a broader distribution in the focal plane than with spherically symmetric illumination. An even larger spread is expected for this profile when the rate k_p in sequential reactions is slow.

In the analysis of photochemical experiments, it may be impractical to work with steady-state conditions because of the accumulation of products and by-products

(Fig. 7A). The asymptotic approach of the averaged spot concentration to a steady state when plotted with $1/\sqrt{t}$ can be used not only to estimate the steady-state concentrations, but also to obtain the reaction and diffusion photolysis parameters. We present calculated results for reactions in the sphere, and results suitable for small cage depletions with Gaussian sphere and cylinder geometries which may be helpful in practical calibrations.

When photolysis proceeds in an enclosed volume such as a cell or an isolated extracellular compartment, diffusional redistribution depends on the relative dimensions of the enclosed space and of the laser spot. For the radius of an enclosing sphere B and radius of spot A, the time to reach 10% of the average spot concentration on the boundary, $t_{10\%}$, is approximately $0.043(B/A)^3\tau$ and is therefore set by geometry and diffusion, not by reaction rate. If we take the optimal duration of photolysis as equal to the diffusional time τ, equating $t_{10\%} = \tau$ determines the *minimal* radius of the closed cell or other structure in which photolysis remains localized, $B_{\min} = 2.85A = 0.856$ μm. Thus, for intracellular photolysis in most cells, with radius exceeding ~0.86 μm, a photolysis duration of τ will result in little product reaching the boundary, whereas for local reaction inside structures smaller than $B_{\min}$, photolysis duration even shorter than τ is required. If the second "dark" step of photolysis was considered, the results might also be scaled by the rate constant k_p in relation to diffusion, as in the results for an infinite medium (model PIM2). It should be noted that $t_{10\%}$ is an arbitrary criterion for localization. Another criterion, the time of maximum concentration gradient between the spot and periphery, $E_{av}(t) - E(B,t)$ (the time of maximum difference between dashed and dotted lines in Fig. 7A), is reached more quickly at fast reaction rates and is proportional to B^2 (data not shown). Experimental parameters controlling product distribution on a sub-micron scale with millisecond resolution are not straightforward to predict, and the data shown in Fig. 7 can be used in the design and interpretation of intracellular photolysis experiments.

It is often the case that the diffusion of products and cage differ substantially because of their relative size and because of local binding to other components. An example is the release of Ca^{2+} ions from DM-nitrophen, DMN-EGTA or NP-EGTA, where Ca^{2+} will diffuse in free solution faster than the caged chelators. Calculations show that when the product is formed by fast "dark" reactions and diffuses faster than the cage, a transient peak of product concentration may develop immediately on photolysis at a high excitation rate k_e, and the steady-state level is reduced by the ratio D_C/D_E relative to the level when both diffusion coefficients are equal to D_C. This provides an explanation for fast Ca^{2+} transients observed on laser photolysis in addition to those involving kinetics of Ca^{2+} rebinding to an unphotolysed cage (Zucker 1993; Ellis-Davies et al. 1996; Escobar et al. 1997). However, the possibility also exists for slowed diffusion of the Ca^{2+} released intracellularly because of repeated binding to cell buffers.

The broad aim of mimicking synaptic action or fast intracellular events by local photolysis requires high photolysis efficiencies to achieve ~0.1–1 mM concentration within a short, 0.1–1 ms, train of laser pulses at non-phototoxic laser intensities. Analysis of toxicity in a synaptic preparation and two-photon photolysis with a nitrophenylethyl cage, described in the following paper (Kiskin et al. 2001), made use of the models and simulations presented here to show that two-photon cross-sections of NPE and similar cages are two to three orders of magnitude too small to be useful in experiments. In addition, the analysis presented here shows that the measured rate constants of "dark" reactions for many commonly used caged compounds are $k_p \ll K_{0.5}$, which makes localization impossible at any excitation rate. Published physiological experiments with two-photon photolysis show small effects of photoreleased substances initiated only with 5–10 ms (Denk 1994) or 25–100 ms (Lipp and Niggli 1998; Furuta et al. 1999) exposures with high laser powers. Such long laser exposures were most likely required for product accumulation because of the low efficiency of uncaging. From these observations and the analysis of reaction with diffusion presented here and in the following paper (Kiskin et al. 2001) it can be concluded that, at present, two-photon photolysis is limited to quasi-steady-state phenomena where exposures are longer than $\tau \approx 100$ μs. The "instant point release" applications, such as simulation of synaptic events, local intracellular Ca^{2+}/second messenger release or high-resolution mapping of cell receptors, require much more efficient photochemistry than is yet available.

Acknowledgements We thank John Corrie, David Trentham, Jim McCray and David Piston for discussions.

References

Altman PL, Dittmer DS (eds) (1972) Biology data book, vol 1, 2nd edn. Federation of American Societies for Experimental Biology, Washington

Brown EB, Shear JB, Adams SR, Tsien RY, Webb WW (1999) Photorelease of caged calcium in femtoliter volumes using two-photon excitation. Biophys J 76:489–499

Brünger A, Peters R, Schulten K (1985) Continuous fluorescence microphotolysis to observe lateral diffusion in membranes. Theoretical methods and applications. J Chem Phys 84:2147–2160

Carslaw HS, Jaeger JC (1959) Conduction of heat in solids, 2nd edn. Oxford University Press, New York

Clements JD (1996) Transmitter timecourse in the synaptic cleft: its role in central synaptic function. Trends Neurosci 19:163–171

Corrie JET, Trentham DR (1993) Caged nucleotides and neurotransmitters. In: Morrison H (ed) Bioorganic photochemistry, vol 2. Wiley, New York, pp 243–305

Crank J (1975) The mathematics of diffusion, 2nd edn. Oxford University Press, New York

Cussler EL (1997) Diffusion, mass transfer in fluid systems, 2nd edn. Cambridge University Press, Cambridge

Denk W (1994) Two-photon scanning photochemical microscopy: mapping ligand-gated ion channel distributions. Proc Natl Acad Sci USA 91:6629–6633

Denk W, Strickler JH, Webb WW (1990) Two-photon laser scanning fluorescence microscopy. Science 248:73–76

Ellis-Davies GC, Kaplan JH, Barsotti RJ (1996) Laser photolysis of caged calcium: rates of calcium release by nitrophenyl-EGTA and DM-nitrophen. Biophys J 70:1006–1016

Escobar AL, Velez P, Kim AM, Cifuentes F, Fill M, Vergara JL (1997) Kinetic properties of DM-nitrophen and calcium indicators: rapid transient response to flash photolysis. Pflugers Arch 434:615–631

Furuta T, Wang SS-H, Dantzker JL, Dore TM, Bybee WJ, Callaway EM, Denk W, Tsien RY (1999) Brominated 7-hydroxycoumarin-4-ylmethyls: photolabile protecting groups with biologically useful cross-sections for two-photon photolysis. Proc Natl Acad Sci USA 96:1193–1200

Kiskin NI, Ogden DC (1998) Diffusion and reaction in extra- and intracellular two-photon photolysis investigated with a caged fluorophore. Biophys J 74:A301

Kiskin NI, Chillingworth R, McCray JA, Piston D, Ogden D (2001) The efficiency of two-photon photolysis of a ''caged'' fluorophore, *o*-1-(2-nitrophenyl)ethylpyranine, in relation to photodamage of synaptic terminals. Eur Biophys J DOI 10.1007/s00249-001-0187-x

Lipp P, Niggli E (1998) Fundamental calcium release events revealed by two-photon excitation photolysis of caged calcium in guinea-pig cardiac myocytes. J Physiol (Lond) 508:801–809

Longsworth LG (1953) Diffusion measurements at 25° of aqueous solutions of amino acids, peptides and sugars. J Am Chem Soc 75:5705–5709

McCollum PA, Brown BF (1965) Laplace transform tables and theorems. Holt, Rinehart and Winston, New York

McCray JA, Trentham DR (1989) Properties and uses of photoreactive caged compounds. Annu Rev Biophys Biophys Chem 18:239–270

Smith GD (1985) Numerical solution of partial differential equations: finite difference methods, 3rd edn. Oxford University Press, Oxford

Xu C, Webb WW (1997) Multiphoton excitation of molecular fluorophores and nonlinear laser microscopy. In: Lakowicz JR (ed) Topics in fluorescence spectroscopy, vol 5. Plenum Press, New York, pp 471–540

Xu C, Zipfel W, Shear JB, Williams RM, Webb WW (1996) Multiphoton fluorescence excitation: new spectral windows for biological nonlinear microscopy. Proc Natl Acad Sci USA 93:10763–10768

Weast RC (ed) (1989) CRC handbook of chemistry and physics, 70th edn. CRC Press, Boca Raton

Zucker RS (1993) The calcium concentration clamp: spikes and reversible pulses using the photolabile chelator DM-nitrophen. Cell Calcium 14:87–100